Pakistan Veterinary Journal

ISSN: 0253-8318 (PRINT), 2074-7764 (ONLINE)
DOI: 10.29261/pakvetj/2025.219

RESEARCH ARTICLE

Dihydrolipoyl Dehydrogenase from *Mycoplasma capricolum subsp. capripneumoniae*: An Immunogenic Plasminogen-Binding Putative Adhesin

Ziqing Wang 1, 2#, Jiazhen Ge 2, 5#, Guodong Song 2, Yijian Liu 2, Qianqian Li 2, Renge Li 2, 5, Pengcheng Gao 2, Fuying Zheng 2*, Yuefeng Chu 1, 2, 3, 4*

[1]College of Veterinary Medicine, Xinjiang Agricultural University, Urumqi 830052, China; [2]State Key Laboratory for Animal Disease Control and Prevention, College of Veterinary Medicine, Lanzhou University, Lanzhou Veterinary Research Institute, Chinese Academy of Agricultural Sciences, Lanzhou 730000, China; [3]Gansu Province Research Center for Basic Disciplines of Pathogen Biology, Lanzhou 730046, China; [4]Key Laboratory of Veterinary Etiological Biology, Key Laboratory of Ruminant Disease Prevention and Control (West), Ministry of Agricultural and Rural Affairs, Lanzhou 730046, China; [5]College of Veterinary Medicine, Gansu Agricultural University, Lanzhou 730070, China.
*Corresponding author: zhengfuying@caas.cn; chuyuefeng@caas.cn

ARTICLE HISTORY (25-368)

Received: April 22, 2025
Revised: July 07, 2025
Accepted: July 14, 2025
Published online: August 19, 2025

Key words:
Adhesin
Dihydrolipoyl dehydrogenase
Mycoplasma capricolum subsp. Capripneumoniae
Plasminogen
Subcellular localization

ABSTRACT

Contagious caprine pleuropneumonia (CCPP), caused by *Mycoplasma capricolum subsp. capripneumoniae* (Mccp), is a severe respiratory disease affecting global goat farming. Mccp infection relies on its adhesion to the host respiratory tract. Dihydrolipoamide dehydrogenase (DLD) is a flavoprotein oxidoreductase that forms disulfide bonds using flavin adenine dinucleotide (FAD). It typically exists as a homodimer, with each 51 kDa subunit covalently linked to one FAD molecule. Although DLD's structure and enzymatic function are well understood, its role in Mccp pathogenicity remains unclear. In our study, rDLD (rMccpDLD) was expressed in *Escherichia coli* BL21(DE3) pLysS and subsequently purified from the supernatant, and mouse antibodies confirmed its presence on the Mccp cell surface. Indirect immunofluorescence showed rMccpDLD binds to GTEC epithelial cells, indicating its role in adhesion. Mouse anti-rMccpDLD serum significantly inhibited M1601 strain adhesion to these cells. Additionally, DLD interacts with host plasminogen, with molecular dynamics simulations confirming stable binding. These results suggest DLD acts as both a virulence factor and adhesin during Mccp infection, making it a potential target for developing new CCPP treatments and vaccines.

To Cite This Article: Wang Z, Ge J, Song G, Liu Y, Li Q, Li R, Gao P, Zheng F, Chu Y 2025. Dihydrolipoylehydrogenase from *Mycoplasma capricolum subsp. capripneumoniae*: an immunogenic plasminogen-binding putative adhesin. Pak Vet J. http://dx.doi.org/10.29261/pakvetj/2025.219

INTRODUCTION

Currently, the management of CCPP is complicated by the diversity of strains and the rise of antibiotic resistance, which underscores the urgent need for new vaccine development. In this context, identifying surface virulence factors in Mccp has emerged as a crucial step toward creating effective vaccines (Jores *et al*., 2020). Therefore, conducting detailed studies on the surface antigens of Mccp and screening for potent protective antigens is essential for overcoming the limitations of current whole-cell inactivated vaccines and paving the way for innovative vaccine solutions.

Mccp primarily establishes itself by colonizing the epithelial cells of the respiratory tract—a process initiated by adhesion, which may help the pathogen evade the host's immune defenses (Iqbal *et al*., 2019). One protein that appears to be key in this interaction is the dihydrolipoamide dehydrogenase (DLD) homologue, which is intimately involved in redox reactions. Notably, similar proteins have been closely linked to cell adhesion in *Mycoplasma synoviae* and *Mycoplasma ovipneumoniae*, demonstrating their potential as vaccine targets (Qi *et al*., 2022; Ge *et al*., 2024). In a similar vein, DLD1 and DLD2 in *Vibrio splendidus* and the membrane protein DLDH in *Streptococcus suis* are also vital for adhesion and the pathogenic process (Pang *et al*., 2015; Dai *et al*., 2019). These findings highlight the significant role of DLD and its homologues in bacterial virulence, presenting them as promising targets for both preventive and therapeutic interventions against CCPP.

Previous research has revealed that the four components of the pyruvate dehydrogenase complex (PDC) in Mccp exhibit immunogenic properties; however, the precise biological functions of these components remain largely uncharted (Zhao *et al*., 2012). Consequently, this study aims to illuminate the role of the PdhD homologue DLD protein—examining its involvement in host cell adhesion, its immunogenicity, subcellular localization, and its interaction with plasminogen.

MATERIALS AND METHODS

Mycoplasma strains, cell lines and culture: The *Mycoplasma capricolum subsp. capripneumoniae* strain is carefully preserved by the Ruminant Bacterial Disease Team at the Lanzhou Veterinary Research Institute (Table 1). These were cultured in an MTB medium made of 21 g/L PPLO broth (BD-Pharmingen, USA), 2 g/L glucose, 20% horse serum, 10% yeast extract, 0.4% phenol red, and 200 U/mL penicillin, adjusted to a pH of 7.8. For colony growth, this medium is solidified with 1.5% agar to create MTA plates.

Recombinant *Escherichia coli* was obtained from monoclonal colonies formed on solid agar medium (Solarbio, China) and then further cultured in LB broth (Solarbio, China) containing 0.1 mg/mL kanamycin (BBI, China).

Goat tracheal epithelial cells (GTEC) are maintained in the cell bank of the Ruminant Bacterial Disease Research Group at the Lanzhou Veterinary Research Institute, Chinese Academy of Agricultural Sciences. Isolated from goat tissues were cultured at 37°C in a 5% CO_2 atmosphere using DMEM/F-12 (Servicebio, China) supplemented with 10% fetal bovine serum (Gibco, New Zealand), 100 U/mL penicillin (HyClone, USA), and 0.1 mg/mL streptomycin (HyClone, USA) (Ge *et al*., 2024).

Bioinformatics analysis: Based on the Mccp DLD sequence template on the indigenous M1601 strain from China (Accession: CP017125 corresponds to the region spanning nucleotides 535434 to 536795). Wecomput supercomputing platform (https://wemol.wecomput) was used to predict its physicochemical properties, and multiple sequence alignments were performed with MAFFT (Duvaud *et al*., 2021; Katoh *et al*., 2005). The mycoplasma strains used in this research are all listed in Table 1. Subsequently, Boltz-1 was employed for tertiary structure prediction and modeling, achieving an accuracy comparable to that of AlphaFold3 (Wohlwend *et al*., 2024). Finally, DiscoTope 3.0 was employed for predicting and visualizing B-cell epitopes and used InterPro to analyze the structural domains (Hoie *et al*., 2024; Blum *et al*., 2025).

Recombinant plasmid construction and recombinant protein purification: Table 2 provides an overview of the primers and plasmids employed in this study. The Mccp DLD gene was chemically synthesized by Wuhan GeneCreate Biological Engineering Co., Ltd. To enhance its expression efficiency in *E. coli*, codon optimization was performed—specifically, converting TGA to TGG. The optimized gene was then inserted into the BamHI and XhoI sites of the pET28a(+) plasmid. The recombinant plasmid into BL21(DE3) pLysS competent cells was introduced via chemical transformation. The transformed cells, carrying the pET28a (+) expression vector, were cultured in LB medium supplemented with 50 μg/mL ampicillin. Finally, the expressed proteins were purified using Ni-NTA affinity chromatography, and their concentration was quantified with the Bicinchoninic Acid (BCA) assay kit (ACE, China).

Table 1: The information of 24 genomes in this study

Name	Identifier	Level	Use in this study
zly1309F	GCA_024758785.1	Complete Genome	Bioinformatics analysis and experiments
Yatta/B	GCA_011464195.1	Complete Genome	Bioinformatics analysis
M1601	GCA_000192395.2	Complete Genome	Bioinformatics analysis and experiments
JF6042	GCA_006970285.1	Complete Genome	Bioinformatics analysis
JF6037	GCA_006969105.1	Complete Genome	Bioinformatics analysis
JF6034	GCA_006970065.1	Complete Genome	Bioinformatics analysis
ILRI181	GCA_000953235.1	Complete Genome	Bioinformatics analysis and experiments
F38	GCA_000953375.1	Complete Genome	Bioinformatics analysis and experiments
Erer	GCA_011464075.1	Complete Genome	Bioinformatics analysis
C550/1	GCA_011464015.1	Complete Genome	Bioinformatics analysis
C5	GCA_011464495.1	Complete Genome	Bioinformatics analysis
Bagamoyo	GCA_011464035.1	Complete Genome	Bioinformatics analysis
AMRC-C758	GCA_011464815.1	Complete Genome	Bioinformatics analysis
9231-Abomsa	GCA_000952915.1	Complete Genome	Bioinformatics analysis
438LP	GCA_011464375.1	Complete Genome	Bioinformatics analysis
2/90	GCA_011464655.1	Complete Genome	Bioinformatics analysis
05021	GCA_011463755.1	Complete Genome	Bioinformatics analysis
04012	GCA_011045555.1	Complete Genome	Bioinformatics analysis
033C1	GCA_011464975.1	Complete Genome	Bioinformatics analysis

Table 2: Plasmids and primers used in this study

Name	Description	Reference
Plasmids		
pET28a-DLD	For expression of recombinant protein His6-PdhD	This study
Primers (5'-3')		
pET28a-DLD-R	GGATCCATGGAAAAGTTCGAT	This study
pET28a-DLD-F	CTCGAGTTATTTGCTTTTAATACCGCG	This study

Preparation of polyclonal antibodies: In this study, six BALB/c mice were initially immunized by a subcutaneous injection that combined complete Freund's adjuvant with 60 μg of the rDLD protein. Two weeks later, the mice received booster shots—administered biweekly—using 60 μg of the rDLD protein mixed with incomplete Freund's adjuvant, totaling three immunizations. Blood was then collected from the orbital sinus to obtain polyclonal antiserum against rDLD, which was later analyzed and characterized using immunoblotting techniques.

All animal care procedures and experiments received approval from the Committee for the Ethics of Animal

Experiments of the Lanzhou Veterinary Research Institute at the Chinese Academy of Agricultural Sciences (LVRIAEC-2022–003).

Localization of DLD in Mccp: To explore the subcellular distribution of Mccp, two types of fractions were prepared specifically: membrane fractions, and cytoplasmic fractions. A membrane and cytoplasmic protein extraction kit from BestBio (Shanghai, China) was used to separate the membrane and cytoplasmic components. After quantifying the protein content with a BCA assay, the concentration of both membrane and cytoplasmic proteins was adjusted to 1 mg/mL using PBS. Immunoblotting with polyclonal antibodies specific to the recombinant protein was then performed.

For the colony hybridization experiments, ~~we~~ the method were followed as described previously (Lan *et al*., 2023). In brief, colony blotting was conducted by gently pressing a Polyvinylidene fluoride (PVDF) membrane onto the Mccp colonies grown on the agar, ensuring that the cell membranes remained intact. The membrane was then blocked with 5% non-fat dry milk. Initially, the membrane was incubated with a mouse anti-DLD polyclonal antibody (diluted 1:10,000), serving as the primary antibody. Subsequently, a goat anti-mouse IgG-HRP secondary antibody (diluted 1:10,000), sourced from Invitrogen (USA), was applied. Finally, the protein signals were visualized using the ECL detection system from Bio-Rad.

Adherence and adherence inhibition assays: The adhesion and adhesion inhibition studies of the DLD protein on GTEC were carried out using an indirect immunofluorescence technique, with some modifications based on previous protocols (Lan *et al*., 2023). First, GTEC cells were plated in 4 mm glass-bottom dishes and cultured for 24 hours. After this incubation period, the cells were blocked using 3% bovine serum albumin (BSA; Sigma) at 37°C for 2 hours. Next, the cells were incubated with either freshly prepared rDLD proteins—dissolving 10 μg per well in 500 μL of DMEM—at 37°C for 1 hour. Cells that did not receive any protein treatment were used as a blank control.

For the adhesion inhibition experiments, Mccp was pretreated at 37°C for 1 hour with either inactivated rDLD mouse polyclonal antiserum or non-immunized mouse serum (both diluted 1:20). This treated Mccp was then added to the GTEC cells at a multiplicity of infection (MOI) of 100. After 4-hours of incubation, the cells were washed three times with PBS and fixed with 4% paraformaldehyde at room temperature for 15 minutes. The samples were subsequently incubated with a goat anti-Mccp polyclonal antiserum (diluted 1:500) at 37°C for 2 hours, followed by a rabbit anti-goat IgG (H + L)-FITC secondary antibody (diluted 1:1,000; Proteintech, USA) at 37°C for 1 hour. Finally, the nuclei were stained with 0.1 μg/mL DAPI (10 μM; Sigma, USA) at room temperature for 10 minutes. The samples were mounted using an antifade medium (Beyotime, China) and then examined under a high-resolution confocal microscope (Ni-U; Nikon).

Interaction between rDLD and GTEC

Experiment on the binding of DLD protein to GTEC membrane proteins: Membrane proteins were isolated from GTEC cells with a Biosharp membrane and cytoplasmic protein extraction kit (China) according to the manufacturer's instructions. To assess the binding of DLD protein to these membrane proteins, a microplate adhesion assay (MPAA) was conducted as described by previous research (Ge *et al.,* 2024; Ma et al., 2024).

For the adhesion assay, a 96-well ELISA plate was coated overnight at 4°C with 100 μL of cell membrane protein at 10, 20, or 40 μg/mL, then blocked with 5% BSA. Next, 100 μL of DLD protein (25 μg/mL) or PBS (control) was added and incubated at 37°C for 2 hours. After washing with PBS-Tween, wells were incubated sequentially with a mouse anti-DLD polyclonal antibody (1:1000) and HRP-conjugated goat anti-mouse IgG (1:10,000). Finally, TMB substrate was added at 37°C for 15 minutes, the reaction was stopped with 2 M H_2SO_4, and the absorbance was measured at 450 nm.

For the adhesion inhibition experiment, a 96-well plate was pre-coated overnight at 4°C with 100 μL of GTEC cell membrane protein (20 μg/mL) and then blocked with 5% BSA at 37°C for 1 hour. Meanwhile, 50 μL of DLD protein (50 μg/mL) was mixed with 50 μL of either anti-DLD serum (from immunized mice) or diluted non-immunized serum (1:20, 1:40, 1:80, or 1:160) and pre-incubated at 37°C for 30 minutes (final DLD concentration: 25 μg/mL). This 100 μL mixture was added to the plate and incubated at 37°C for 2 hours and then processed as in the adhesion assay.

Binding experiment of rDLD protein and plasminogen: Plasminogen activation assay was performed as described by (Ge *et al.,* 2024). Briefly, plasminogen (Abcam, UK) at 5 μg/mL in 0.05 M carbonate buffer (pH 9.6) was added to a 96-well ELISA plate and incubated overnight at 4°C. The next day, after washing with PBST, the plate was blocked with 5% BSA at 37°C for 2 hours. Then, different concentrations of rDLD protein (6.25–100.0 μg/mL) or PBS (negative control) were added and incubated at 37°C for 2 hours. After further washing, mouse anti-His monoclonal antibody (1:10,000) was added for 1 hour at 37°C, followed by HRP-conjugated goat anti-mouse IgG (1:10,000) for another hour. The reaction was developed with TMB for 10 minutes in the dark at room temperature, stopped with 2 M H_2SO_4, and the absorbance was measured at 450 nm.

Molecular Docking and Molecular Simulation of rDLD Protein and Plasminogen: Molecular docking and molecular dynamics (MD) simulations were performed to study the binding mechanism between rDLD and plasminogen (Plg). The 3D structure of Plg was obtained from the PDB (4DUR). Using pyDockWEB, rDLD was docked as the ligand to Plg (receptor) via rigid-body blind docking over the entire molecular surface (Jimenez-Garcia et al., 2013). Electrostatic and desolvation scores were employed to evaluate binding affinity, and a two-dimensional interaction map was generated using the Wecomput platform.

For MD simulations, the docked rDLD–Plg complex was used as the starting structure in Gromacs 2024 (Van Der Spoel *et al*., 2005; Lemkul, 2024). The simulation system comprised the TIP3P water model and 0.15 M NaCl to mimic physiological conditions. After energy

minimization (5000 steps each of steepest descent and conjugate gradient), the system was heated to 300 K under NVT conditions (100 ps) and equilibrated under NPT conditions (500 ps). A 100-ns production run was then carried out at 300 K and 1 atm with a 2-fs time step, saving trajectory data every 10 ps. The SHAKE algorithm constrained hydrogen bonds, and AMBER 03 force field parameters were used. Finally, RMSD, RMSF, and radius of gyration analyses were performed to assess the complex's stability.

Statistical Analysis: All experiments were independently repeated three times with each sample analyzed in triplicate. Statistical analyses were performed using Origin 2024 software with non-paired t-tests and one-way or two-way ANOVA. Significant differences were marked as follows: *P<0.05, **P<0.01, ***P<0.001 and ****P<0.0001; "ns" indicates no significance.

RESULTS

Bioinformatics analysis of DLD sequences and B-cell epitopes: The work started from analyzing the physicochemical properties of the DLD protein using ExPASy from Wecomput, as detailed in Table 3. The protein weighs roughly 51 kDa and has an isoelectric point of 8.476. In conditions without disulfide bonds, its molar extinction coefficient measures 30,830 $M^{-1}cm^{-1}$ (equivalent to 0.603 L $g^{-1}cm^{-1}$), and it rises slightly to 31,080 $M^{-1}cm^{-1}$ (or 0.608 L $g^{-1}cm^{-1}$) when disulfide bonds are present. An instability index of 28.06 suggests that DLD is quite stable, while an aromaticity value of 0.095 and a GRAVY score of -0.06 indicate its propensity toward hydrophilicity. A closer look at its secondary structure reveals that about 37.5% is composed of α-helices, 21.2% forms β-sheets, and 20.3% consists of turns. Moreover, under standard physiological conditions the net charge registers at +3.658, confirming that the protein carries a slight positive charge at around pH 7. These characteristics collectively hint at its inherent stability and hydrophilic nature, factors that likely contribute to its biological function and interactions.

Table 3: Protein physico-chemical properties of DLD

Sequence ID	DLD
Molecular Weight	51144.711
Isoelectric Point	8.476
Molar Extinction Coefficient (without disulfide bond)	30830
Extinction Coefficient (without disulfide bond)	0.603
Molar Extinction Coefficient (with disulfide bond)	31080
Extinction Coefficient (with disulfide bond)	0.608
Instability Index	28.06
Aromaticity	0.095
Grand average of hydropathicity (GRAVY)	-0.06
Helix Fraction	0.375
Turn Fraction	0.203
Sheet Fraction	0.212
Net Charge	3.658

Further sequence analysis of the DLD protein revealed some fascinating insights. A multiple sequence alignment performed using MAFFT showed remarkable conservation, with a nucleotide sequence that is 100% similar within the species (Fig. 1A). To visualize its structure, a three-dimensional model was constructed using the Boltz-1 algorithm. The model achieved a high confidence score of 0.9396, underscoring its reliability (Fig. 1B). In addition, B-cell epitopes predicted using DiscoTope 3.0 highlighted several regions (marked in red) that could potentially serve as antigenic sites, reflecting the protein's excellent immunogenic properties (Fig. 1C). Finally, a domain analysis conducted with the InterPro tool provided deeper insight into the functional roles of the DLD protein (Fig. 1D).

Surface localization analysis of Mccp-DLD protein: Recombinant proteins, along with their corresponding polyclonal antisera, were successfully obtained (Fig. 2A). Using previously described methods, cell membrane and cytoplasmic proteins from four Mccp strains were extracted F38, M1601, ILRI181, and zly1309F (Fig. 2B)—and then analyzed them by Western blot. The results revealed a distinct band at approximately 54 kDa in both the cell membrane and cytoplasmic fractions of Mccp (dual His-tag), indicating that the DLD protein is present in both cellular compartments.

To further confirm the distribution of DLD within intact cells, a colony hybridization approach was employed. Mccp colonies with intact membranes showed clear bands when hybridized with DLD-specific polyclonal antibodies. In contrast, no bands were observed using negative control antibodies. These findings confirm the dual localization of the DLD protein on Mccp cells (Fig. 2C).

rMccp-DLD plays a part-time role of adhesion as an adhesive of Mccp: Using laser confocal microscopy, direct adhesion of rMccp-DLD to GTEC cells was observed (Fig. 3A). In contrast, when pre-immune serum was used, there was no noticeable specific binding. To further explore the role of surface-exposed DLD on Mccp in mediating cell adhesion, an antibody inhibition assay was conducted using laser confocal microscopy. The results were striking: when anti-DLD serum was applied, the number of Mccp bacteria attaching to goat GTEC cells dropped significantly compared to the pre-immune serum group (Fig. 3B). This finding strongly supports the idea that surface-localized DLD is key to the adhesion process.

Furthermore, the binding affinity between recombinant DLD (rDLD) and GTEC cell membrane proteins was quantitatively assessed through the application of a microtiter plate adhesion assay (MPAA). The data showed a pronounced binding affinity between DLD and the membrane proteins (P<0.001). Notably, as the concentration of rDLD increased, OD450 values rose in a clear dose-dependent manner (Fig. 3C). When anti-DLD serum was introduced, this binding was markedly inhibited compared to the pre-immune serum treatment (Fig. 3D; P<0.0001).

rDLD binds to the host's plasminogen: A microtiter plate assay was conducted to evaluate the binding capacity of rDLD to Plg. The data revealed that wells incubated with Plg displayed a noticeably higher optical density at 450 nm compared to the control wells (P<0.0001) (Fig. 4A). Additionally, as the concentration of rDLD increased, so did the OD450 readings, suggesting dose-dependent binding behavior.

In parallel, molecular docking results are shown in Fig. 4B, with Table 4 detailing the computed outcomes from pyDockWEB—including electrostatic, desolvation,

and van der Waals forces. These analyses indicate a favorable binding affinity between Plg and rDLD, with significant interactions observed at positions 96, 100 and 408 of rDLD (Fig. 4C).

Molecular simulation demonstrated that rDLD binds to the host's plasminogen to form a stable complex: Molecular dynamics (MD) simulations were run. using Gromacs 2024 to explore the conformational stability of the complex formed between rDLD and host plasminogen over a 100-nanosecond period. To assess system stability and amino acid mobility, the simulation trajectories was analyzed by calculating both the root-mean-square deviation (RMSD) and root-mean-square fluctuation (RMSF) (Fig. 5A and 5B). Herein, findings from one representative simulation are presented, as two independent runs yielded highly similar results.

Table 4: Predicted binding energies (kcal/mol) of Plg/DLD protein complexes

Binding energies (kcal/mol)	Plg/DLD
Electrostatics	-23.762
Desolvation	-26.079
VdW	41.544
Total	-45.686

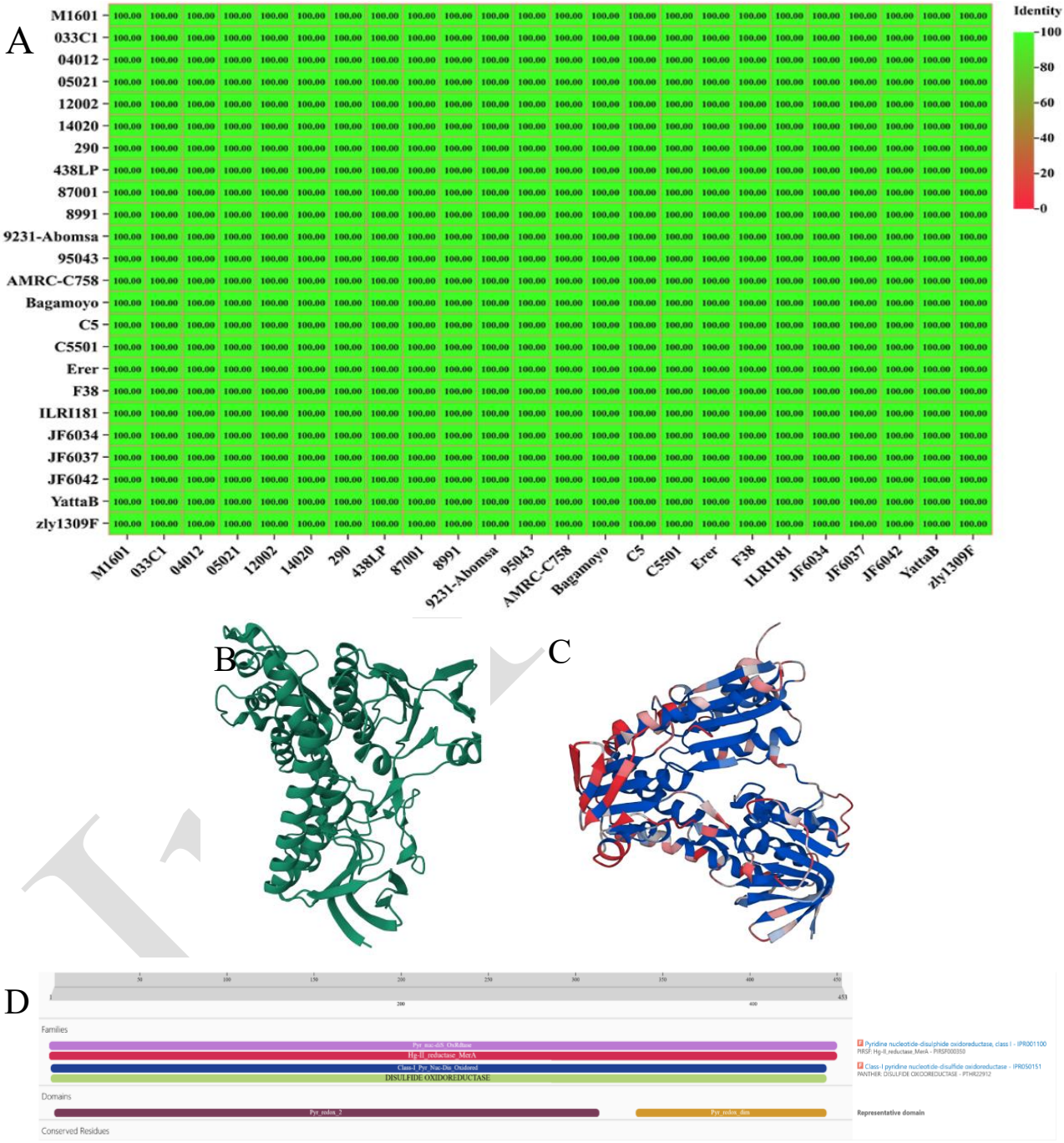

Fig. 1: Bioinformatics analysis of DLD sequences and B-cell epitopes. (A) Multiple sequence alignment using MAFFT shows complete (100%) conservation of the DLD gene within the species. (B) The three-dimensional structure model of DLD, generated by the Boltz-1 algorithm, displays a high confidence score (0.9396), supporting its reliability. (C) B-cell epitope prediction using DiscoTope 3.0 highlights several potentially antigenic regions (highlighted in red), indicating strong immunogenic potential. (D) Domain analysis performed with the InterPro tool reveals functional domains within DLD, providing insight into its biological roles. The physicochemical properties detailed in Table 3 further support the protein's stability and hydrophilic nature.

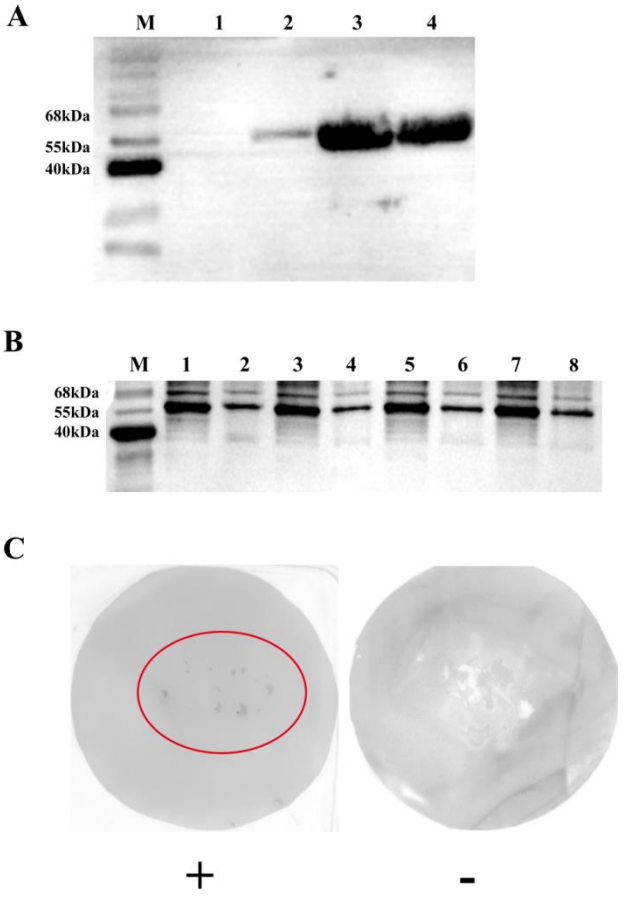

Fig. 2: Surface localization analysis of the Mccp-DLD protein. (A) Expression and purification of recombinant DLD protein and its corresponding polyclonal antisera are shown. Lane 1 represents the sample before induction, lane 2 represents the sample after induction, lane 3 represents the sample before purification, and lane 4 represents the sample after purification. (B) Western blot analysis of cell membrane and cytoplasmic fractions from four Mccp strains (F38, M1601, ILRI181, and zly1309F) demonstrates the presence of a ~54 kDa band in both compartments, confirming dual localization. Specifically, lanes 1 and 2 correspond to the cell membrane and cytoplasmic fractions of strain F38, respectively; lanes 3 and 4 correspond to those of strain M1601; lanes 5 and 6 correspond to those of strain ILRI181; and lanes 7 and 8 correspond to those of strain zly1309F. M stands for protein marker. (C) Colony hybridization using DLD-specific polyclonal antibodies yields clear bands on intact Mccp colonies, whereas no bands appear with negative control antibodies, further validating the dual cellular distribution of DLD (+ indicates incubation of positive serum; - indicates incubation of negative serum.).RMSD served as our main marker for determining when the complex reached equilibrium. After roughly 25 nanoseconds, the rDLD-plasminogen complex began to stabilize, with the overall fluctuations settling into a narrow range between 0.8 nm and 1.0 nm (Fig. 5A).

Subsequently, the RMSF was examined to gauge the stability of individual amino acid residues throughout the simulation. The RMSF profiles of the complex showed nearly identical trends, with only minor differences detected likely reflecting slight variations in binding affinity. Importantly, the RMSF values for most residues remained below 0.6 nm, a relatively low figure that implies a high level of rigidity and dynamic stability compared to similar studies (Fig. 5B).

Additionally, the radius of gyration (Rg) of the complex was evaluated to assess its compactness. The Rg values showed minimal fluctuation during the simulation, stabilizing between 3.9 and 4.1 nm (Fig. 5C). This consistent range suggests that the complex maintained good flexibility and structural cohesion throughout the simulation.

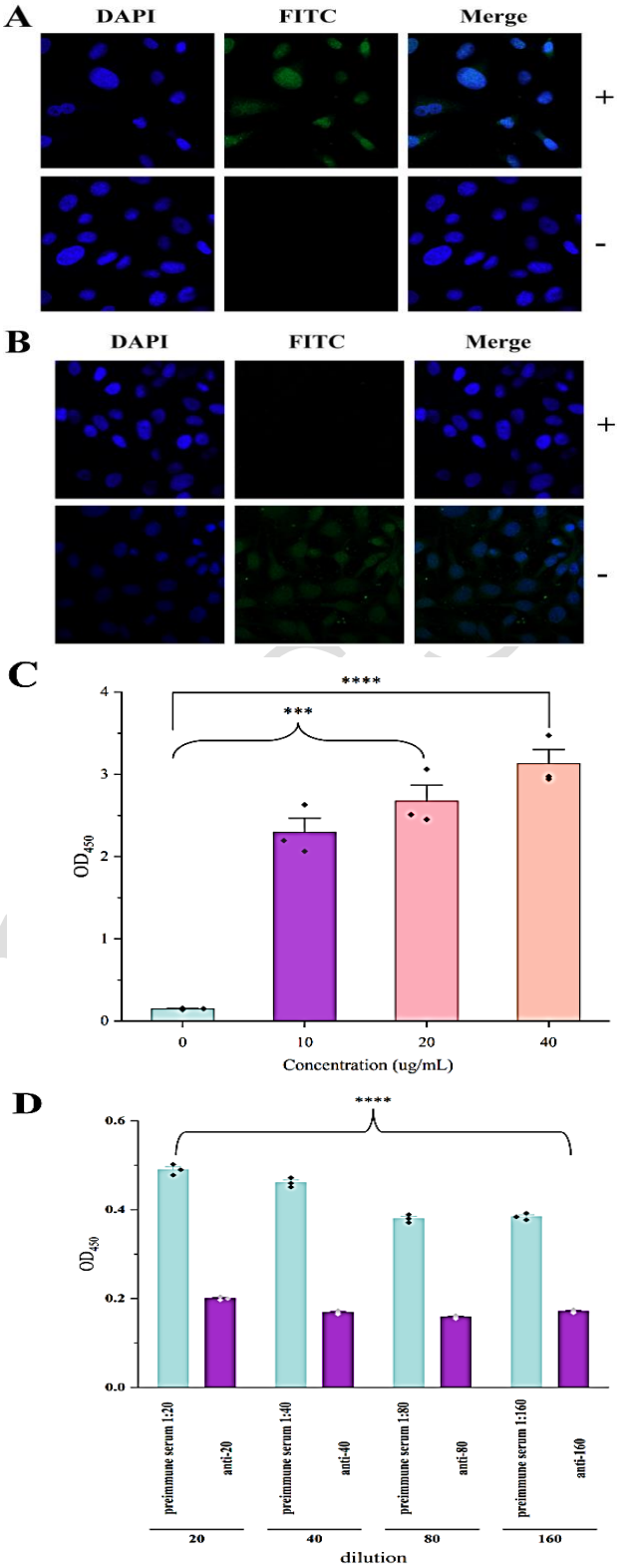

Fig. 3: Role of rMccp-DLD in mediating adhesion. (A) Laser confocal microscopy images reveal direct adhesion of rMccp-DLD to GTEC cells, while pre-immune serum shows no specific binding (+ indicates incubation of positive serum; - indicates incubation of negative serum). (B) Antibody inhibition assay via confocal microscopy indicates a significant reduction in the attachment of Mccp to goat GTEC cells when treated with anti-DLD serum compared to pre-immune serum, highlighting the role of surface-localized DLD (+ indicates incubation of positive serum; - indicates incubation of negative serum.). (C) A microtiter plate adhesion assay (MPAA) quantitatively demonstrates a dose-dependent binding between rDLD and GTEC cell membrane proteins as evidenced by increasing OD450 values. (P<0.001) (D) Inhibition of binding by anti-DLD serum, compared with pre-immune serum (P<0.0001), further confirms the adhesive function of DLD.

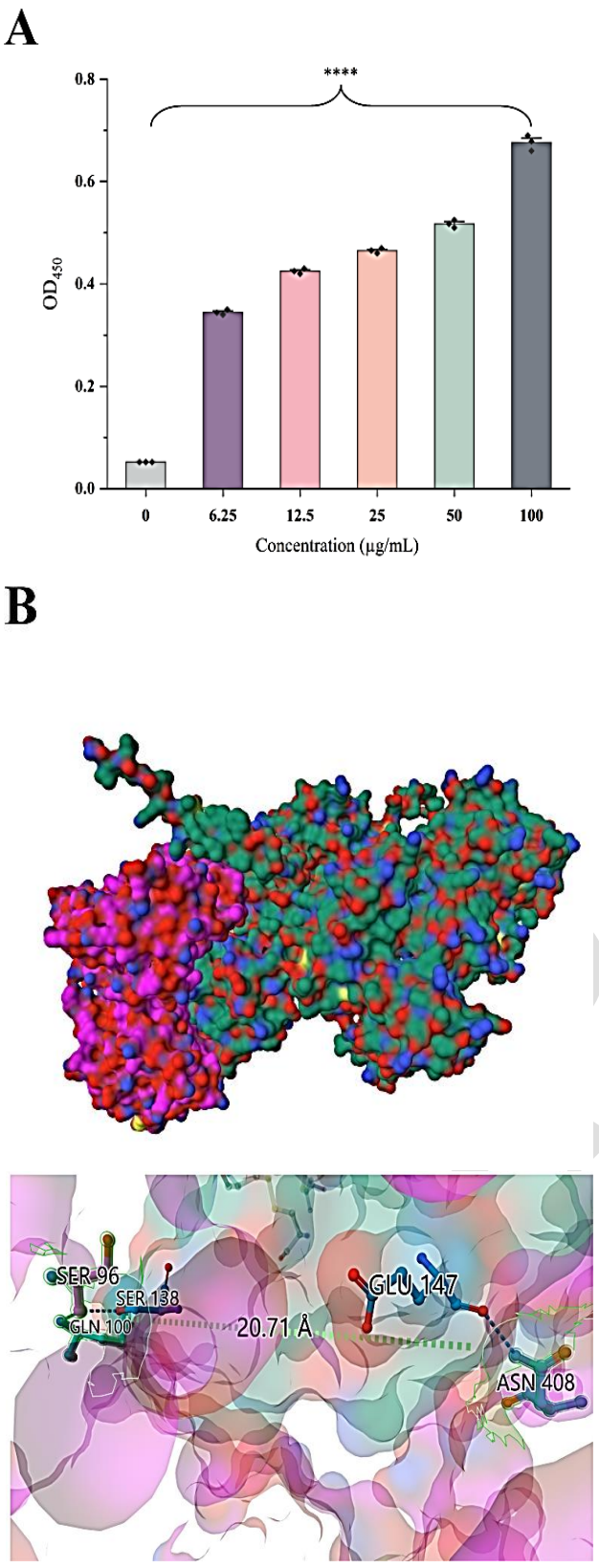

Fig. 4: rDLD binds to host plasminogen. (A) A microtiter plate assay shows that wells incubated with plasminogen exhibit significantly higher OD450 readings compared to controls (P<0.0001), with binding increasing in a dose-dependent manner as rDLD concentration rises. (B) Molecular docking results depict the interaction interface between rDLD and plasminogen (Pink represents DLD protein and green represents plg). (C) Detailed analysis from pyDockWEB (refer to Table 1) identifies key interaction sites at positions 96, 100 and 408 of rDLD, underscoring a favorable binding affinity driven by electrostatic, desolvation, and van der Waals forces (Pink represents DLD protein and green represents plg).

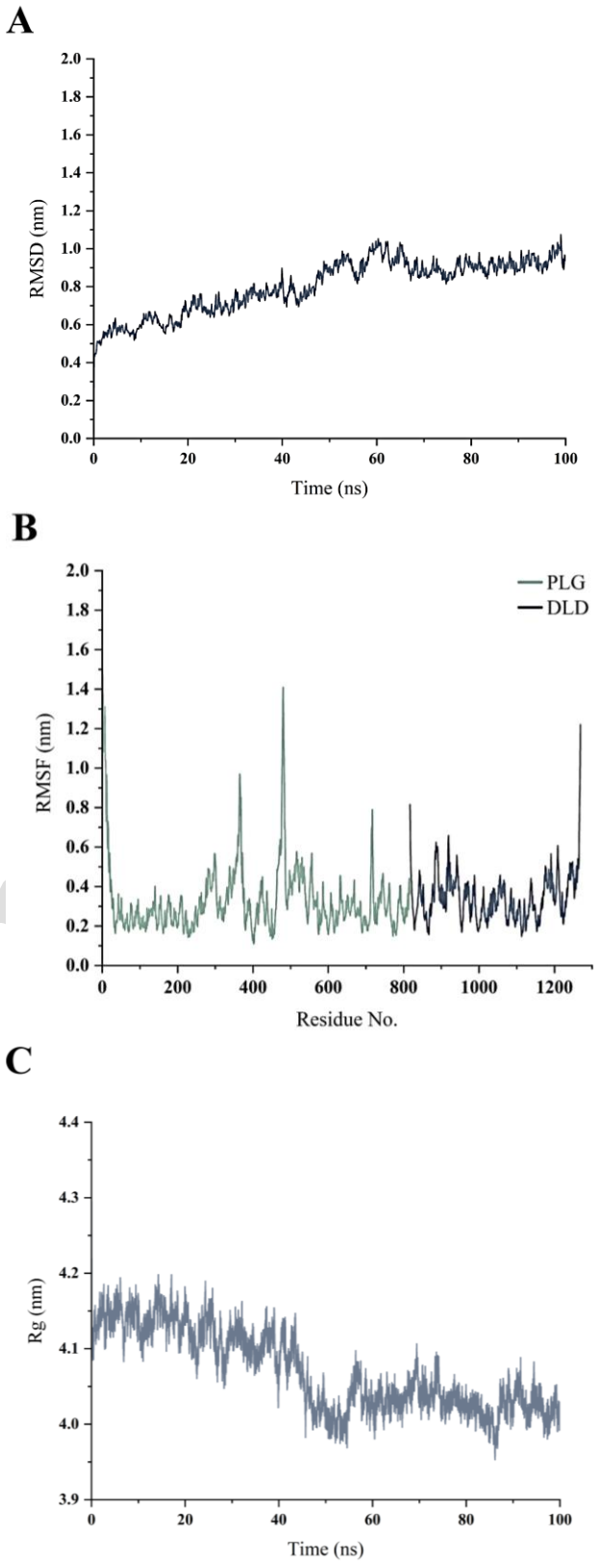

Fig. 5: Molecular dynamics simulation of the rDLD–plasminogen complex. (A) The root-mean-square deviation (RMSD) plot. (B) Root-mean-square fluctuation (RMSF) analysis. (C) The radius of gyration (Rg) profile.

DISCUSSION

Understanding the interactions between *Mycoplasma capricolum subsp. capripneumoniae* (Mccp) and its host is crucial for developing effective vaccines and therapeutic

strategies. During infection, Mccp relies on several critical factors—including adhesion, invasion, and immune evasion—to survive and multiply within the host. Adhesion and colonization mark the first steps of infection, and the genes involved are often seen as promising targets for vaccines and drug development. For example, research has found that genes linked to cell adhesion frequently mutate in attenuated mycoplasma strains, underscoring the importance of adhesion mechanisms in pathogenicity (Li *et al*., 2020; Zhu *et al*., 2020). Worldwide, Mccp causes significant economic losses in the goat industry, yet our limited understanding of its pathogenic mechanisms continues to hamper vaccine development (Jiang *et al*., 2017; Bai *et al*., 2020; Rahman *et al*., 2024). Earlier studies have only predicted a few virulence proteins and a handful of prominent immunogenic proteins using bioinformatics approaches (Yatoo *et al*., 2019; Li *et al*., 2020). Therefore, identifying protective antigens remains an essential step in the development of an anti-Mccp vaccine. In this study, it was confirmed that DLD not only localizes to the Mccp membrane but also plays a key role in facilitating adhesion to host respiratory epithelial cells.

DLD is a versatile oxidoreductase integral to bacterial metabolism. It primarily functions in the tricarboxylic acid cycle and branched-chain amino acid metabolism (De Kok *et al*., 1998). As a key component of the pyruvate dehydrogenase and α-ketoglutarate dehydrogenase complexes, DLD catalyzes the oxidation of dihydrolipoamide to lipoamide and transfers electrons to NAD^+, generating NADH and driving energy metabolism along with ATP synthesis (Yi *et al*., 2021). Interestingly, in some mycoplasmas, DLD exhibits adhesin-like properties (Qi *et al*., 2022; Ge *et al*., 2024). Given the challenges posed by heterogeneity in developing vaccines and therapeutics against mycoplasmas, identifying conserved virulence proteins is particularly important (Akhtar *et al*., 2022; Lorenzon *et al*., 2002). Multiple sequence alignments reveal that DLD is uniquely conserved among mycoplasmas, and its stability index and hydrophilicity suggest that it can persist stably within cells and participate in diverse biological processes. The evaluation of the B-cell epitopes of DLD protein was conducted using DiscoTope-3.0, which demonstrated that this protein has excellent antigenic properties. The structure domain of the protein was predicted based on sequence analysis using Interpro, and its potential role in DLD was predicted. These findings highlight its potential as a vaccine target.

In this study, DLD localization in both the cell membrane and cytoplasm of Mccp was confirmed through techniques including Western blotting and colony hybridization. This dual localization not only indicates its role in metabolism but also points to its importance in mediating interactions between Mccp and host cells. Similar dual roles have been reported for other mycoplasma virulence proteins (Li *et al*., 2022; Qi *et al*., 2022; Ge *et al*., 2024). Moreover, protein adhesion assays and antibody inhibition experiments further supported the essential role of surface-exposed DLD in mediating host cell adhesion, consistent with the previously reported adhesive functions of DLD (Qi *et al*., 2022; Ge *et al*., 2024). It appears that DLD may facilitate adhesion through high-affinity binding to host cell membrane proteins, opening new avenues for antibacterial strategies that target DLD.

Molecular docking is a computational method that predicts the binding sites and affinities between proteins, revealing the molecular mechanism of their interactions. It usually employs rigid or flexible docking algorithms to scan the molecular surfaces and evaluate the binding energies (Zhao *et al*., 2025; Jiang *et al*., 2025). Molecular dynamics simulation, on the other hand, simulates the dynamic behavior of protein complexes under physiological conditions to analyze their structural stability, flexibility, and dynamic changes in interactions, providing in-depth insights in the temporal dimension for the binding mechanism (Honma and Suzuki, 2023; Gasparello *et al*., 2023). The combination of these two methods can comprehensively analyze the molecular basis of protein interactions and lay the foundation for studying their biological functions. In the study of the interaction between DLD and plasminogen, pyDockWEB was used to scan the entire molecular surface to identify binding sites, and charge and desolvation scoring was employed to evaluate the binding affinity. Meanwhile, molecular dynamics simulation based on Gromacs simulated the dynamic behavior of the protein complex under physiological conditions to verify its stability. These methods not only deeply analyzed the molecular mechanism of DLD and plasminogen but also laid the foundation for understanding their roles in pathogen infection. Through molecular docking and molecular dynamics simulation, it was found that there might be a stable interaction between DLD and plasminogen. This interaction might help Mccp invade and disseminate within the host by activating the plasminogen system, which could degrade the extracellular matrix and enhance infectivity (Lan *et al*., 2023). These findings offer additional insights into how DLD may contribute to the pathogenicity of Mccp by facilitating its invasive processes.

Despite some advances made in this study, limitations remain. Although our simulations have demonstrated an interaction between rDLD and plasminogen, further validation through mutation analysis and binding kinetics experiments is necessary. Jores et al. identified five research priorities for CCPP vaccine development: 1) detailed characterization of surface-localized virulence factors; 2) development of mutants and confirmation of attenuation in standardized caprine ex vivo models; 3) evaluation of these mutants in vivo for both attenuation and immune response induction; 4) determination of immunological correlates of protection—through adoptive transfer of caprine IgG from immunized animals and thorough characterization of both innate and adaptive immune responses after infection; and 5) application of systems immunology to refine the adjuvant formulations used in current bacterin vaccines (Jores *et al*., 2020). This study represents only a preliminary step in characterizing these virulence factors. Future work should focus on constructing and validating mutant strains, assessing in vivo immune responses, and optimizing adjuvants. Furthermore, given the current limitations in genetic manipulation systems for mycoplasmas, there is an urgent need for the development of effective genetic tools-a challenge that require concerted international collaboration.

Conclusions: In summary, the present study highlights the vital role of the DLD protein in mediating interactions between Mccp and its host, as demonstrated through a blend of bioinformatics, molecular simulations, and experimental validation. It has been confirmed that DLD is not only an antigenic protein present on the surface of the Mccp cell membrane but is also highly conserved and stable. Beyond its well-established roles in metabolism and cellular functions, DLD appears to facilitate pathogen invasion by aiding adhesion to host respiratory epithelial cells and binding to host plasminogen. These findings shed fresh light on the pathogenic mechanisms of Mccp and its interactions with the host, paving the way for the development of targeted prevention and treatment strategies.

Acknowledgements: This work was supported by grants from the National Key Research and Development Program of China (2022YFD1800704) and the Major Science and Technology Project of Gansu Province (23ZDNA007). We are grateful to associate research fellow Huafang Hao of Lanzhou Veterinary Research Institute, Chinese Academy of Agricultural Sciences, for providing the GTECs. We are grateful to Wuhan Genecreate Biological engineering Co., Ltd. for assisting in gene synthesis.

Conflict of Interest: The author(s) declare no conflict of interest.

Authors contribution: ZW and JG experiment, data analysis and the initial draft of the manuscript; GS animal experiments and assisted in data organization; YL data analysis; QL protein expression and purification; RL animal experiments; YX, WW and PG experimental procedures; FZ and YC guidance on research design, supervised the experimental process, revised the manuscript, and performed the final review.

REFERENCES

Akhtar A, Boissiere A, Hao H, *et al*., 2022, Multi-locus sequence analysis reveals great genetic diversity among *Mycoplasma capricolum subsp. capripneumoniae* strains in Asia. Vet Res 53, 92.

Blum M, Andreeva A, Florentino LC, *et al*., 2025. InterPro: The protein sequence classification resource in 2025. Nucleic Acids Res 53:D444-D456.

De Kok A, Hengeveld A F, Martin A, *et al*., 1998, The pyruvate dehydrogenase multi-enzyme complex from Gram-negative bacteria. Biochim Biophys Acta 1385, 353-366.

Dai F, Zhang W, Zhuang Q, *et al*., 2019. Dihydrolipoamide dehydrogenase of *Vibrio splendidus* is involved in adhesion to Apostichopus japonicus. Virulence 10:839-848.

Duvaud S, Gabella C, Lisacek F, *et al*., 2021, Expasy, the Swiss Bioinformatics Resource Portal, as designed by its users. Nucleic Acids Res 49, W216-W227.

Gasparello, J, Verona, M, Chilin, A, *et al*., 2023, Assessing the interaction between hemoglobin and the receptor binding domain of SARS-CoV-2 spike protein through MARTINI coarse-grained molecular dynamics. Int J Biol Macromol 253, 127088.

Ge J, Tian T, Liu Y, *et al*., 2024. *Mesomycoplasma (Mycoplasma) ovipneumoniae* dihydrolipoamide dehydrogenase is an immunogenic plasminogen binding protein and a putative adhesin. Vet Microbiol 299:110302.

Hoie MH, Gade FS, Johansen JM, *et al*., 2024. DiscoTope-3.0: Improved B-cell epitope prediction using inverse folding latent representations. Front Immunol 15:1322712.

Honma M, Suzuki H, 2023, Can molecular dynamics facilitate the design of protein-protein-interaction inhibitors? Nat Rev Rheumatol 19, 8-9.

Iqbal Yatoo M, Raffiq Parray O, Tauseef Bashir S, *et al*., 2019. Contagious caprine pleuropneumonia – A comprehensive review. Vet Q 39:1-25.

Jiang L, Zhang K, Zhu K, *et al*., 2025, From Traditional Methods to Deep Learning Approaches: Advances in Protein–Protein Docking. Wiley interdisciplinary reviews. Computational molecular science 15.

Jimenez-Garcia B, Pons C, Fernandez-Recio J., 2013, pyDockWEB: a web server for rigid-body protein-protein docking using electrostatics and desolvation scoring. Bioinformatics 29, 1698-1699.

Jores J, Baldwin C, Blanchard A, *et al*., 2020. Contagious Bovine and Caprine Pleuropneumonia: A research community's recommendations for the development of better vaccines. NPJ Vaccines 5:66.

Katoh K, Kuma K, Toh H, *et al*., 2005, MAFFT version 5: improvement in accuracy of multiple sequence alignment. Nucleic Acids Res 33, 511-518.

Lan S, Li Z, Hao H, *et al*., 2023. A genome-wide transposon mutagenesis screening identifies LppB as a key factor associated with *Mycoplasma bovis* colonization and invasion into host cells. FASEB J 37:e23176.

Lemkul JA, 2024. Introductory Tutorials for Simulating Protein Dynamics with GROMACS. J Phys Chem B 128:9418-9435.

Li L, Luo D, Liao Y, *et al*., 2020. *Mycoplasma genitalium* Protein of Adhesion induces inflammatory cytokines via Cyclophilin A-CD147 activating the ERK-NF-κB pathway in human urothelial cells. Front Immunol 11:2052.

Li Y, Wang J, Liu B, *et al*., 2022. DnaK functions as a moonlighting protein on the surface of *Mycoplasma hyorhinis* cells. Front Microbiol 13:842058.

Li Y, Wang R, Sun W, *et al*., 2020, Comparative genomics analysis of *Mycoplasma capricolum subsp. capripneumoniae* 87001. Genomics 112, 615-620.

Lorenzon S, Wesonga H, Ygesu L, *et al*., 2002, Genetic evolution of *Mycoplasma capricolum subsp. capripneumoniae* strains and molecular epidemiology of contagious caprine pleuropneumonia by sequencing of locus H2. Vet Microbiol 85, 111-123.

Ma H, Zhao Y, He X, *et al*., 2024, Dihydrolipoamide acetyltransferase is a key factor mediating adhesion and invasion of host cells by *Mycoplasma synoviae*. Vet Microbiol 299, 110297.

Pang H, Chen L, Zhang Y, *et al*., 2015. Construction and biological function analysis of a dldh deletion mutant strain of *Vibrio alginolyticus*. Agric Biotechnol 4:47-51.

Qi J, Wang Y, Li H, *et al*., 2022. *Mycoplasma synoviae* dihydrolipoamide dehydrogenase is an immunogenic fibronectin/plasminogen binding protein and a putative adhesin. Vet Microbiol 265:109328.

Rahman M H, Alam M.S, Ali M.Z, *et al*., 2024, First report of contagious caprine pleuropneumonia (CCPP) in Bangladeshi goats: Seroprevalence, risk factors and molecular detection from lung samples. Heliyon 10, e40507.

Van Der Spoel D, Lindahl E, Hess B, *et al*., 2005. GROMACS: Fast, flexible, and free. J Comput Chem 26:1701-1718.

Wohlwend J, Corso G, Passaro S, *et al*., 2024. Boltz-1 Democratizing Biomolecular Interaction Modeling. bioRxiv.

Yatoo MI, Parray OR, Bhat RA, *et al*., 2019. Novel candidates for vaccine development against *Mycoplasma capricolum subspecies capripneumoniae* (Mccp) – Current knowledge and future prospects. Vaccines 7.

Yi L, Fan Q, Wang Y, *et al*., 2021, Evaluation of immune effect of *Streptococcus suis* biofilm-associated protein PDH. Vet Microbiol 263, 109270.

Zhao G, Zhang Y, Li Y, *et al*., 2025, Design of multi-epitope chimeric phage nanocarrier vaccines for porcine deltacoronavirus. Vet Microbiol 304, 110487.

Zhao P, He Y, Chu Y, *et al*., 2012. Identification of novel immunogenic proteins in *Mycoplasma capricolum subsp. capripneumoniae* strain M1601. J Vet Med Sci 74:1109-1115.

Zhu X, Baranowski E, Dong Y, *et al*., 2020. An emerging role for cyclic dinucleotide phosphodiesterase and nanoRNase activities in *Mycoplasma bovis*: Securing survival in cell culture. PLoS Pathog 16:e1008661.